ELSEVIER

Review and comparison of approaches to proton exchange membrane fuel cell modeling

Denver Cheddie, Norman Munroe *

Mechanical and Materials Engineering, CEAS 2441, Florida International University, 10555W Flagler Street, Miami, FL 33174, USA

Abstract

A review of recent literature on proton exchange membrane fuel cell modeling is presented. Fuel cell models can be categorized as analytical, semi-empirical or mechanistic. Mechanistic models can be further subcategorized based on the solution strategy, single-domain or multi-domain. The multi-domain approach develops and solves separate equations in each region of the fuel cell. The single-domain approach consists of equations governing the entire domain of interest, with source and sink terms accounting for species consumption and generation within the cell. The merits and demerits of each method are discussed. For a one-dimensional case study, both methods were compared quantitatively and results show that both models accurately predict the polarization effects and water management requirements.
© 2005 Elsevier B.V. All rights reserved.

Keywords: Proton; Exchange; Fuel; Cell; Mechanistic; Modeling

1. Introduction

It is believed that there will be a time in the future when global energy demands will be met by some source other than fossil fuels. It is believed that hydrogen will play a major role in such a future [1]. The concept of a hydrogen economy describes an economy where the principal source of energy is hydrogen related. Fuel cells, in particular proton exchange membrane fuel cells (PEMFC), are expected to play a major role in a future hydrogen economy. Fuel cells are particularly attractive for use in vehicles as a replacement to the combustion engine. The low temperature operation of a PEMFC (typically <90 °C) allows for easy start up and quick response to changes in load and operating conditions.

However, a number of issues need to be resolved before fuel cells can be commercially viable. Typical proton exchange membranes require precise water management, which is difficult under the variable load associated with automobile driving conditions. Dehydration of the membrane results in

lower ionic conductivity as well as the risk of de-adhesion of the membrane, whereas excessive water production (at high current densities) results in mass transport limitations on the cathode side. Sluggish electrode kinetics also poses a problem. The rate of oxygen reduction at the cathode is much slower than hydrogen oxidation at the anode, and this limits the performance of the cell. Also, trace amounts of carbon monoxide in the hydrogen feed have a deleterious effect on the platinum based catalyst typically used in PEMFCs.

Fuel cell modeling has received much attention over the past 15 years in an attempt to better understand the phenomena occurring within the cell. Parametric models allow engineers and designers to predict the performance of the fuel cell given geometric parameters, material properties and operating conditions, such as temperature, pressure and humidity. Such models are advantageous because experimentation is costly and time consuming. Furthermore, experimentation is limited to designs, which already exist, thus does not facilitate innovative design. Given the highly reactive environment within the fuel cell, it is often impossible to measure critical parameters, such as temperature, pressure and potential gradients, or species concentration within the cell. Thus, detailed

---

* Corresponding author. Tel.: +1 305 348 3556; fax: +1 305 348 6142.
  E-mail addresses: dched002@fiu.edu (D. Cheddie), munroen@fiu.edu
(N. Munroe).

Nomenclature

a	effective catalyst surface area per unit volume (m^{-1})
c	concentration $(mol\,m^{-3})$
C_1, C_2	integration constants
D_i	diffusion constant of species i $(m^2\,s^{-1})$
$D_{i,j}$	diffusivity of gas pair $i-j$ in a mixture $(m^2\,s^{-1})$
E	potential (V)
f	F/RT (V^{-1})
F	Faraday's constant (C equivalent^{-1})
i	ionic current density $(A\,m^{-2})$
I	cell current density $(A\,m^{-2})$
k_p	hydraulic permeability (m^2)
k_φ	electro-kinetic permeability (m^2)
K_i	Henry's law constant for species i $(Pa\,m^3\,mol^{-1})$
P	pressure (Pa)
R	universal gas constant $(J\,mol^{-1}\,K^{-1})$
T	temperature (K)
v	pore water velocity $(m\,s^{-1})$
v_s	superficial water velocity $(m\,s^{-1})$
x_i	mole fraction of species i
z_i	charge number of species i

Greek letters

α_a, α_c	anodic and cathodic transfer coefficients
γ	concentration parameter in Butler–Volmer equation
$\varepsilon_{i,k}$	volume fraction of species i in region k
ζ	stoichiometric flow ratio
κ	ionic conductivity of the membrane $(mho\,m^{-1})$
μ	pore water dynamic viscosity $(kg\,m^{-1}\,s^{-1})$
ρ	water molar density $(mol\,m^{-3})$
σ	electrical conductivity $(mho\,m^{-1})$
φ	potential (V)

transport models, which accurately predict the flux and concentration of multiple species are required. Such information is useful, for example, in the loading of catalysts. Transport models can be used to predict the pH within the cell in order to identify the optimum operating conditions for certain catalysts, and also to identify where most of the electrochemical reactions take place. The performance of ceramic-based catalysts is pH dependent. Transport models can determine the pH in the catalyst regions based on the H^+ concentration. This would help designers to optimize the cell for effective catalyst usage and utilization.

This paper reviews some of the work done in PEMFC modeling over the past 15 years, discusses contemporary trends and compares various approaches to modeling in recent times.

2. Categories of fuel cell models

A fuel cell model may fall into one of three categories: analytic, semi-empirical, or mechanistic (theoretical). Table 1 categorizes the models reviewed in this paper according to their areas of investigation and dimension of study.

2.1. Analytical models

Examples of analytical modeling are those reported by Standaert et al. [2,3]. Many simplifying assumptions were made concerning variable profiles within the cell in order to develop an approximate analytical voltage versus current density relationship. This model also predicted water management requirements. This was done in the case of isothermal and non-isothermal cells. However, analytical models are only approximate and do not give an accurate picture of transport processes occurring within the cell. They are limited to predicting voltage losses and water management requirements for simple designs. They may be useful if quick calculations are required for simple systems.

2.2. Semi-empirical models

Semi-empirical modeling combines theoretically derived differential and algebraic equations with empirically determined relationships. Empirical relationships are employed when the physical phenomena are difficult to model or the theory governing the phenomena is not well understood. Springer et al. [4] developed a semi-empirical model for use in a fuel cell with a partially hydrated membrane (as opposed to a fully hydrated membrane). Empirically determined relationships were developed correlating membrane conductivity and electrode porosity with water content in the Nafion® membrane. Most of the models subsequently developed used these correlations to determine the conductivity of the Nafion® membrane.

Amphlett et al. [5] used semi-empirical relationships to estimate the potential losses and to fit coefficients in a formula used to predict the cell voltage given the operating current density. This model accounted for activation and ohmic overpotentials. The partial pressures and dissolved concentrations of hydrogen and oxygen were determined empirically as a function of temperature, current density and gas channel mole fractions. Subsequently, the reversible cell voltage, activation overpotentials and cell resistance were correlated with temperature, partial pressures, dissolved concentrations and operating current density. Pisani et al. [6] also used a semi-empirical approach to study the activation and ohmic losses as well as transport limitations at the cathode reactive region.

Maggio et al. [7] studied the water transport in a fuel cell using a semi-empirical approach. They modeled the concentration overpotential effect by allowing the cathode

Table 1
PEMFC model categorization based on areas of investigation

Feature	Analytical		Semi-empirical						Mechanistic																					
	2	3	4	5	6	7	8	9	10	11	12	14	16	17	18	19	20	21	22	23	24	25	26	27	28	29	30	31	32
Dimension									1	1	2	3	3	1	2	3	3	3	3	1	2	2	3	3	3	2	3	3	3
Polarization	√	√	√	√	√	√	√	√	√	√	√	√	√	√	√	√	√	√	√	√	√	√	√	√	√	√	√	√	√
Transport phenomena											√	√	√	√	√	√	√	√	√	√	√	√	√	√	√	√	√	√	√
Thermal effects																			√	√	√	√							
Water management									√	√											√	√							
Concentration effects					√										√	√													
CO kinetics							√										√												
Catalyst utilization									√	√																			
Flow field effects																						√	√	√	√	√	√	√	√
Membrane conductivity			√																										
FC stacks								√													√								

gas porosity to be an empirical function of current density (since current density is related to water production). The effective gas porosity was assumed to decrease linearly with increasing current density. This is due to the increasing percentage of gas pores occupied by liquid water. Their results indicate that dehydration of the membrane is likely to occur on the anode side rather than the cathode side.

Chan et al. [8] studied the effect of CO kinetics in the hydrogen feed on the anode reactive region. When hydrogen is obtained from reformed fuel, there are trace amounts of CO present which act as poison to the platinum catalyst. The CO is preferentially adsorbed onto the catalyst surface instead of hydrogen, whereby decreasing the catalyst surface area available for hydrogen dissociation. An empirical factor was determined which represented the fraction of catalyst sites occupied by CO at the anode. The result is larger activation overpotentials on the anode side due to slow electrode kinetics.

Semi-empirical modeling has also been used to model fuel cell stacks. Maxoulis et al. [9] used such an approach to model a fuel cell stack during automobile driving cycles. They combined the model of Amphlett et al. [5] with the commercial software ADVISOR, which was used to simulate vehicular driving conditions. They studied the effects of the number of cells per stack, electrode kinetics and water concentration in the membrane on the fuel consumption. They concluded that a larger number of cells per stack result in greater stack efficiency resulting in better fuel economy.

Semi-empirical models are, however, limited to a narrow corridor of operating conditions. They cannot accurately predict performance outside of that range. They are very useful for making quick predictions for designs that already exists. They cannot be used to predict the performance of innovative designs, or the response of the fuel cell to parameter changes outside of the conditions under which the empirical relationships were developed. Empirical relationships also do not provide an adequate physical understanding of the phenomena inside the cell. They only correlate output with input.

2.3. Mechanistic models

Mechanistic modeling has received the most attention in the literature. In mechanistic modeling, differential and algebraic equations are derived based on the physics and electro-chemistry governing the phenomena internal to the cell. These equations are solved using some sort of computational method. Mechanistic models can be subcategorized as multi-domain models or single-domain (or unified) models. Fig. 1 gives a chronology of the development of mechanistic modeling. It shows the evolution of PEMFC modeling as it increased in complexity.

2.3.1. Multi-domain approach

Multi-domain models involve the derivation of different sets of equations for each region of the fuel cell, namely the anode and cathode gas diffusion regions, anode and cathode gas flow channels, membrane and catalyst layers. These equations are solved separately and simultaneously.

One of the early mechanistic models for a PEMFC was the pioneering work of Bernardi and Verbrugge [10,11]. They developed a one-dimensional, steady state, isothermal model which described water transport, reactant species transport, as well as ohmic and activation overpotentials. Their model assumed a fully hydrated membrane at all times, and thus calculated the water input and removal requirements to maintain full hydration of the membrane. The model equations were derived using the Stefan Maxwell equations to describe gas phase diffusion in the electrode regions, the Nernst–Planck equation to describe dissolved species fluxes in the membrane and catalyst layers, the Butler Volmer equation to describe electrode rate kinetics and Schlogl's equation for liquid water transport.

This model was used primarily to predict the polarization effects (due to ohmic and activation overpotentials) and the water management requirements. The model computed the required water input at the anode side and required water removal rate at the cathode side necessary to maintain full hydration of the Nafion® membrane at all times.
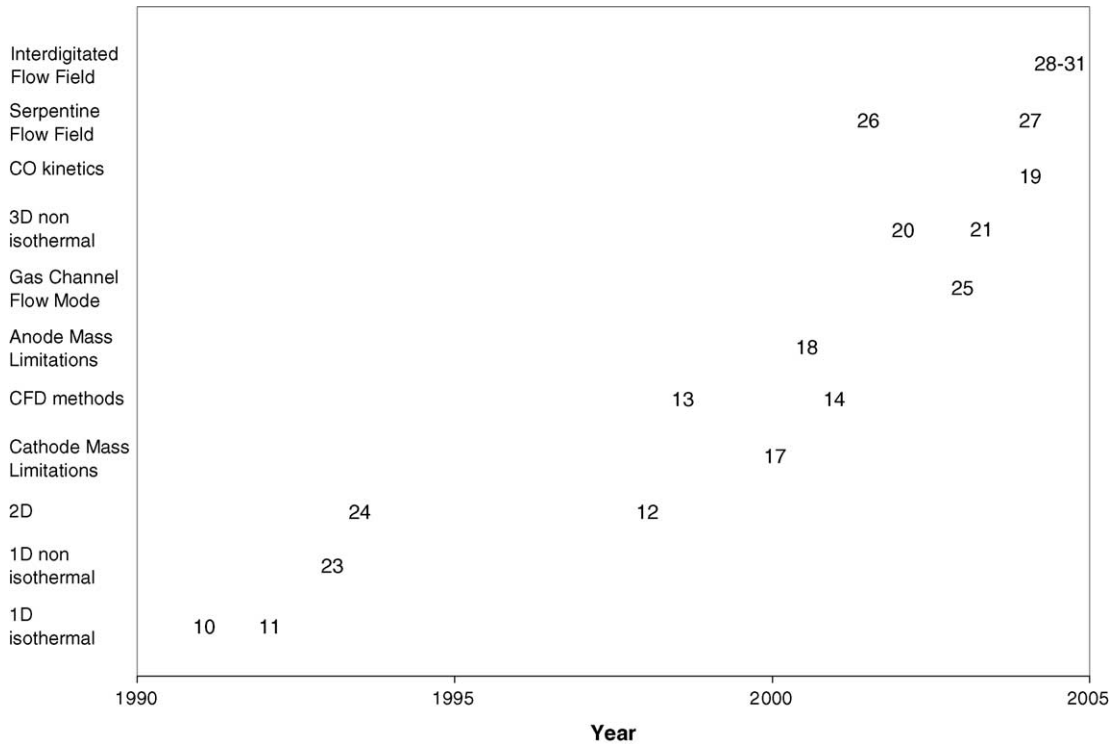
Fig. 1. PEMFC mechanistic modeling evolution.

Their model also predicted the dissolved hydrogen and oxygen concentrations within the catalyst layers and it was found that at sufficiently high current densities most of the electrochemical reactions occurred on the outer surface of the catalyst layer. This information is vital to designers of fuel cells. It allows them to economically distribute the catalyst where it is most needed. Considering that the platinum catalyst is one of the largest expenses in a fuel cell, this could help reduce the cost. Although their model was basic and many improvements have been made since, this work served as a foundation for PEMFC modeling.

Gurau et al. [12] developed a two-dimensional model to determine species concentrations within the fuel cell and the effect on fuel cell performance of gas diffuser porosity, air flow rates in the gas channel and temperature. This model is based on the multi-domain approach with three domains considered: gas diffusers/gas flow channels, catalyst layers and membranes. The gas diffusers and gas flow channels were combined into one domain by writing the governing equations for each region in a similar form. As a result the solution methodology was able to accommodate both regions into one domain.

2.3.2. Single-domain approach

Gurau et al. [12] showed that since the governing differential equations in the gas flow channels and the gas diffusion electrodes are similar, the equations can be combined for both regions. The computational effect is that both regions can be considered as one domain where no internal boundary con-

ditions or statements of continuity need be defined. The only difference is that material properties and source terms assume different values for the two regions. This forms the basis of the single-domain approach.

Instead of combining two regions into one domain, the single-domain approach combines all the regions of interest into one domain. Conservation equations are defined which govern the entire domain of interest, typically the entire fuel cell (gas flow regions and the membrane electrode assembly). In each region, the differences are accounted for by source and sink terms. All equations are written in the form of a generic convection–diffusion equation, and all terms, which do not fit that format are dumped into the source or sink term. This formulation allows for solution using known computational fluid dynamics (CFD) methods.

The principles of CFD were first applied to fuel cells by Wang et al. [13] and Zhou and Liu [14]. In the unified approach, all the governing differential equations were arranged into a standard form, which could be discretized using the principles of CFD [15] or solved using a CFD software package.

$$\frac{\partial \Phi}{\partial t} = \nabla(v\Phi) + \nabla(\Gamma\nabla\Phi) + S$$

The respective terms in above equation represent transient, convection, diffusion and source. The general variable may refer to potential, temperature, pressure, velocity, concentration or phase fraction. For steady state operation the transient term vanishes. This general equation is a conservation equation, where the source term represents material consumption

and generation (at catalyst layers), phase change and any other term, which cannot fit the general format, but must be accounted for. The application of CFD to fuel cells has paved the way for the subsequent development of multidimensional models.

3. Modeling considerations

Mechanistic modeling (single and multi-domain) has been utilized to study a wide range of phenomena including polarization effects (activation, ohmic and concentration overpotentials), water management, thermal management, CO kinetics, catalyst utilization and flow field geometry.

3.1. Parametric models

All models are parametric in that they predict the output performance for various input parameters, typically temperature, pressure and humidity. Wang et al. [16] developed a three-dimensional parametric model, considering the effects of temperature, humidity and pressure. It was found that the performance of the fuel cell improved with increasing temperature if the inlet gases are fully humidified. If the gases are not fully humidified, dehydration of the membrane is likely to occur resulting in reduced conductivity values, hence reduced cell performance. They also found that at low current densities anode humidification is required, but not at higher current densities. This is because at high current densities, sufficient water is produced at the cathode to keep the membrane hydrated.

Their results further show that cathode humidification is not significant at all, especially at high current densities. This is because dehydration is likely to occur on the anode side and flooding on the cathode side. Therefore, humidifying the cathode gas stream adds no benefit.

Finally, increasing the pressure of the inlet gases was seen to improve performance by increasing the activation currents and the partial pressures of reactant gases.

The authors report that at higher current densities, their model overestimates the cell current density compared to experimental results. The reason for this is that the model did not take into account mass transport effects.

3.2. Mass transport effects

Mass transport limitations or concentration overpotentials are caused when the reactants cannot be supplied fast enough for the required rate of chemical reaction to take place. This happens especially at high current densities when large amounts of liquid water are produced at the cathode. Liquid water has a two-fold effect. It dilutes the reactants thus reducing its concentration near the catalyst sites, and it reduces the effective gas porosity thus "blocking" the reactants from reaching the catalyst layer.

Baschuk and Li [17] developed a one-dimensional model, which accounted for cathode mass limitation effects by allowing variable degrees of flooding at the cathode catalyst layer/backing region. They account for concentration overpotential as a result of the decreased concentration of dissolved oxygen in the catalyst region due to the excessive water content. Darcy's law is used to obtain the drop in partial pressure of the oxygen at the cathode catalyst layer, and Henry's law is used to determine the dissolved oxygen concentration. Their modeled results showed excellent agreement with experimental results. The model also predicted that increasing the cell pressure lowers the limiting current density. High pressures result in maximum flooding occurring at lower current densities, and this effect is more significant than the increase in partial pressure of the oxygen. The results also showed, predictably, that increasing the temperature increases the limiting current density.

Um et al. [18] developed a transient model based on the unified approach, which studied the effects of hydrogen dilution along the anode gas channel. The two-dimensional model considered flow perpendicular to the membrane electrode assembly (MEA) cross-section, as well as in the direction of flow in the gas channels. As hydrogen diffuses from the gas channel into the gas diffusion region, its concentration along the gas channel decreases resulting in a two-dimensional concentration gradient in the gas diffusion electrodes. The result is that mass transport limitations are seen on the anode side especially at high current densities, and when reformed fuel is used instead of pure hydrogen. At high current densities, hydrogen is extracted from the flow channels at a much fast rate than at low current densities. With reformed fuel, the partial pressure of the hydrogen is already lowered by the presence of carbon dioxide in the gas feed, so as it is used up toward the end of the gas channel, the partial pressure of the hydrogen may be too low and it may not be able to diffuse to the anode catalyst layer fast enough. The result is anode side mass transport limitations. Such phenomena cannot be studied using one-dimensional models.

Zhou and Liu [19] developed a 3-D model of a PEMFC taking into account CO effects in the anode gas stream. The model accounts for poisoning of the catalyst as well as hydrogen dilution due to the inert gases. An interesting result is that along the anode gas channel the hydrogen concentration increases in the direction of flow because the CO is depleted at a faster rate due to preferential adsorption at the catalyst sites. They also found that the optimum porosity of the gas diffusion layer is much lower for a fuel cell using reformate than one using pure hydrogen.

3.3. Thermal management

The electrochemical reactions taking place in a fuel cell are exothermic, i.e., they give off heat. Heat is also produced by irreversibilities in the cell such as activation losses and ohmic effects. Heat removal is a critical design issue for fuel cells. Excessive heat generation may result in dehydration of

the membrane resulting in decreased conductivity, and thermal stresses resulting in mechanical failure. Various models have accounted for non-isothermal effects and heat transfers.

Berning et al. [20,21] used the unified approach to develop a three-dimensional non-isothermal fuel cell model. The model studied reactant concentrations, current density distributions and temperature gradients within the cell as well as water flux and species transport. For gas flow fields separated by current collecting plates, three-dimensional effects were observed due to the unevenness of the hydrogen and oxygen supply. These effects were pronounced under the collector plate land areas. These effects may result in transport limiting conditions at high current densities.

The development of a non-isothermal model was intended to study the heat transfers within the cell. It was observed that a temperature difference of 2–3 K existed within the cell. Yan et al. [22] performed a similar study and found a temperature variation within the cell of the same magnitude. However, the magnitude of the heat transfer was not reported so it is difficult to compare the magnitude of the conductive heat transfer relative to the total heat transfer. This information would have helped justify the need for non-isothermal modeling. If the heat transfer by conduction were small compared to other heat transfers, then a temperature difference of 2–3 K could hardly be significant.

Wohr et al. [23] investigated heat management for fuel cell stacks. In their one-dimensional, non-isothermal model they considered the gas diffusion region to be a homogeneous distribution of cylindrical pores, through which transport was governed by the "dusty gas model". Water transport in the electrodes was assumed to occur by surface diffusion or capillary effect. They considered the heating effects due to ohmic resistance in the membrane and heat generation due to the entropy of reaction. In the absence of any heat removal strategy, the temperature difference in a stack of four cells was 8 K. The temperatures of the innermost cells in the stack were the highest. The effect is that the membranes of the inner cells would dehydrate.

3.4. Water management

Water management is another critical aspect of PEM fuel cells. At high current densities, excessive water transport across the membrane and water production at the cathode result in flooding of the electrodes and mass transport limitations. At low current densities, dehydration of the membrane may occur at the anode side. Water must be supplied to the fuel cell at the anode and removed at the cathode in order to maintain effective membrane humidification.

The Bernardi and Verbrugge model [10,11] determines the required water addition and removal necessary to maintain full membrane humidification at a given current density. Fuller and Newman [24] developed a pseudo two-dimensional model, which predicted water and thermal management as well as fuel utilization for a fuel cell operating with reformed methanol as the fuel.

The model of Wohr et al. [23] showed that for fuel cell stacks water management becomes even more difficult and is strongly related to thermal management. The temperatures of the inner cells of the stack are higher than the outer cells resulting in membrane dehydration. Water management is strongly interrelated with thermal management/heat removal. Other strategies for effective water management involve the geometry of the gas flow field, e.g., counter flow versus co-flow, and using serpentine and interdigitated flow fields rather than straight channel flow fields.

3.5. Flow field geometry

One of the advantages of computational modeling over experimentation to assess the performance of a fuel cell is the ability to evaluate innovative designs. One area where this is evident is in the consideration of flow field geometry. Models have been developed for straight flow channels, serpentine flow channels and interdigitated flow fields.

Ge and Yi [25] developed a two-dimensional model to study the effects of flow mode in straight gas channels, i.e., counter flow versus co-flow. It was found that the flow mode only made a difference when dry or low humidity inlet gases were used. For such cases, counter flow operation produced better results since by so doing the reactant gases were sufficiently humidified internally. If the inlet gases are already humidified, the flow mode makes little difference. The reason for this is that for high humidity gases, the increase in membrane conductivity due to the high humidity is counteracted by the increase in cathode concentration overpotential due to the presence of liquid water. This is the case whatever the flow mode. However, for low humidity gases, counter flow operation allows for internal humidification of the gas streams. For co-flow low humidity gases, the membrane dehydrates. This information gives the designers of fuel cells an alternative to humidifying the gas streams.

Dutta et al. [26] used the unified approach to study mass transport between the channels of a PEMFC with a serpentine flow field. Their model is three-dimensional and allows for multi-species transport. They studied the effect of flow channel width in the serpentine flow field on velocity distribution, gas mixture distribution and reactant consumption. Serpentine flow fields allow for a greater area for diffusion of the supply gases. Their results show that for low humidity conditions, water transport is dominated by electro-osmotic effects, i.e., water flows from anode to cathode at the side of the cell closer to the gas channel inlet. At the outlet side of the cell, water transport is dominated by back diffusion, and it flows in the opposite direction. Thus the serpentine flow field allows for circulation of the water within the cell.

Nguyen et al. [27] developed a three-dimensional model which accounts for mass and heat transfer, current and potential distribution within a cell using a serpentine flow field. Their results show that oxygen concentration along the gas channels decrease in the direction of flow. Also, in the gas diffusion layer, the oxygen concentration is a minimum under

the land area. At high current densities the oxygen is almost completely depleted under the land areas. The result is an uneven distribution of oxygen concentration along the catalyst layer resulting in local overpotentials, which vary spatially. A unique feature of this model is a voltage-to-current (VTC) algorithm, which allows for the solution of the potential field and the local activation overpotential. Since the reactant concentration is not constant across the catalyst layer, the activation overpotential will not be constant. Their simulations show a variation in local activation overpotential from 0.31 to 0.37 V at a current density of $1.2\,\mathrm{A\,cm^{-2}}$. This VTC algorithm however, comes with a computational cost. It slows down the solution requiring 6000–8000 iterations for convergence.

Um and Wang [28] used a three-dimensional model to study the effects an interdigitated flow field. The model accounted for mass transport, electrochemical kinetics, species profiles and current density distribution within the cell. Interdigitated flow fields result in forced convection of gases, which aids in liquid water removal at the cathode. This would help improve performance at high current densities when transport limitations due to excessive water production are expected. The model shows that there is little to no difference at low to medium current densities between an interdigitated flow field and a conventional flow field. However, at higher current densities, a fuel cell with an interdigitated flow field has a limiting current, which is nearly 50% greater than an equivalent cell with a conventional flow field. Because of the flow field, three-dimensional effects under the current collector land area, known as rib effects, are prominent.

Seigel et al. [29] also modeled a fuel cell with an interditated flow field. Theirs was a two-dimensional steady state model, which studied transport limitations due to water build up in the cathode catalyst region. They considered water in three phases: liquid, gas and dissolved (membrane phase). They found that treating the catalyst layer as a very thin interface underestimates the transport limitations due to water build-up. Hence, they modeled the catalyst layer as a finite region. Their model showed that 20–40% of the water building up at the cathode catalyst layer comes from water which is transported across the membrane. This problem may be counteracted by applying a pressure differential to force back diffusion of water, i.e., from cathode to anode.

Using the multi-domain approach Hu et al. [30,31] developed a three-dimensional two-phase model for a fuel cell. They gave boundary conditions, which could be used for straight flow channels as well as interdigitated flow fields. Unlike previous models, which assume separate flow channels for gases and liquids, this model assumes a two-phase mixture. Water properties such as specific volume change depending on the degree of mixture. They used a CFD algorithm to solve for the flow field in the gas flow channels and diffusion regions, and the fourth order Runge–Kutta method together with a shooting technique to solve for the flow field in the catalyst layers and the membrane.

For the interdigitated flow field, results show that the oxygen concentration is higher and liquid water saturation is lower than those for a conventional straight channel flow field. The higher oxygen concentration results in fast reaction rates and the lower liquid water saturation results in less concentration overpotential. It is also shown that the local current densities are much more uniform with an interdigitated flow field than with a conventional flow field. However, the performance of a fuel cell with an interdigitated flow field is only shown to be better than that for one with a conventional flow field if the inlet gases are well humidified. This is because the interdigitated field aids in water removal, but does not aid in hydration of an already de-hydrated membrane. So, the internal gases need to be humidified.

Using the unified approach, Kumar and Reddy [32] studied the effects of having metal foam in the flow field of the bipolar plates. Their three-dimensional steady state model shows that decreasing the permeability of the gas flow field improves performance. This is because at low flow field permeability reactant gases are transported by forced convection rather than diffusion. Having many tiny gas channels results in a lower permeability than having few large channels. However, due to limitations in machining processes, the flow channels cannot be made too small. Placing metal foam in the flow field allows the flow field permeability to be lowered without resorting to precise machining processes. They found that decreasing the permeability from 10^{-6} to $10^{-12}\,\mathrm{m^2}$ increases the "average current density" of their system from 5943 to $8425\,\mathrm{A\,m^{-2}}$.

4. Comparisons

In this section, we compare the unified (single-domain) approach with the multi-domain approach to solving the governing equations. In Section 3, we saw that both approaches have been used to solve three-dimensional problems with very complex flow fields. The early mechanistic models were all solved using the multi-domain approach. With the introduction of CFD methods to fuel cell modeling, the door opened for multi-dimensional modeling. Most of the models developed over the past 5 years were solved using the single-domain approach.

Although both approaches have been used for multidimensional models, the single-domain approach more easily lends itself to multidimensional modeling. With the multi-domain approach, internal boundary conditions or conditions of continuity must be specified at each interface between regions, which could become cumbersome in two- and three-dimensions.

The single-domain approach also more easily lends itself to be implemented in commercial CFD codes since the solution methods to CFD problems are well established. The solution methods for the multi-domain equations are not as standardized as those for the single-domain equations. As a

result, the model development time is shortened using the single-domain approach.

An interesting observation is that many of the earlier models developed by researchers with a chemical engineering/chemistry background were based on the multi-domain approach, whereas most of the newer models developed by researchers with a mechanical engineering background are based on the unified approach.

It is difficult to say which method converges faster since that depends heavily on what is being modeled, and how efficiently the programs are written. It has been reported that the single-domain approach requires longer solution times [29], however, a possible reason is that commercial codes are very general and not computationally optimized for any specific situation.

5. Case study

For the purpose of comparison, we solved the model developed by Bernardi and Verbrugge [11] using both approaches. The same terminology as employed by the authors [11] is used together with the same material properties and operating conditions. The model is one-dimensional, the only dimension considered is that perpendicular to the MEA cross section. The solution domain consists of the MEA, i.e., the anode and cathode gas diffusion regions, catalyst layers and the membrane. The assumptions of the model are:

- constant cell temperature (isothermal), in this case 353 K;
- ideal and well-mixed gases in the gas chambers;
- steady state operation;
- total gas pressure within each diffuser region is taken to be constant since gas phase viscosity is small compared to liquid phase viscosity;
- inlet gas streams (hydrogen and air) are saturated and gases are assumed to be fully saturated throughout the cell;
- separate flow channels for gases and liquids in the porous regions of the gas diffusion layers, i.e., liquid and gas phases will be treated as separate single phase flows rather than a two phase mixture.

The Nernst–Planck equation is used to describe the transport of dissolved species in the membrane and catalyst layers. Transport of dissolved species occurs via diffusion, convection and migration. Schlogl's equation is used to describe the transport of liquid water via electro-osmotic drag and back diffusion. The Stefan Maxwell equations are used to describe the diffusion of gases within the gas diffusion regions. The Butler–Volmer equation is used to describe electrochemical rate kinetics in the catalyst layers.

5.1. Multi-domain approach

The multi-domain model is characterized by equations (1)–(25) in each region as reported in [11]. Note that in these equations, the current density, I, assumes a positive value. In the anode gas diffusion region:

$$N_{H_2} = \frac{I}{2F} \tag{1}$$

$$N_w = \frac{I}{2F} \left(\frac{p_w^{sat}}{p_0 - p_w^{sat}} \right) \tag{2}$$

$$\frac{d\phi_{solid}}{dz} = -\frac{I}{\sigma_d^{eff}} \tag{3}$$

$$\frac{dp}{dz} = -\frac{\mu}{k_p^d} v_s \tag{4}$$

In the cathode gas diffusion region:

$$N_{O_2} = -\frac{I}{4F} \tag{5}$$

$$N_w = -\frac{I}{4F} x_w \left[1 - x_w + x_{N_2} \left(\frac{D_{w,O_2}^{eff}}{D_{w,N_2}^{eff}} - 1 \right) \right]^{-1} \tag{6}$$

$$\frac{dv_s}{dz} + \frac{1}{\rho} \frac{dN_w}{dz} = 0 \tag{7}$$

$$\frac{d\phi_{solid}}{dz} = -\frac{I}{\sigma_d^{eff}} \tag{8}$$

$$\frac{dp}{dz} = -\frac{\mu}{k_p^d} v_s \tag{9}$$

$$\frac{dx_{N_2}}{dz} = x_{N_2} \frac{RT}{p_L} \left(\frac{N_{O_2}}{D_{O_2,N_2}^{eff}} + \frac{N_w}{D_{w,N_2}^{eff}} \right) \tag{10}$$

In the membrane:

$$D_{H_2} \frac{d^2 c_{H_2}}{dz^2} - v \frac{dc_{H_2}}{dz} = 0 \tag{11}$$

$$D_{O_2} \frac{d^2 c_{O_2}}{dz^2} - v \frac{dc_{O_2}}{dz} = 0 \tag{12}$$

$$N_{H^+} = \frac{I}{F} \tag{13}$$

$$\frac{dp}{dz} = -\frac{\mu}{k_p} v_s + \frac{k_\phi}{k_p} z_f c_f F \frac{d\phi}{dz} \tag{14}$$

$$\frac{d\phi}{dz} = \frac{I - Fc_f v}{-\kappa} \tag{15}$$

In the cathode catalyst layer:

$$\frac{dv_s}{dz} = -\frac{1}{2\rho F} \frac{di}{dz} \tag{16}$$

$$\frac{dp}{dz} = -\frac{\mu}{k_p^{eff}} v + \frac{k_\phi^{eff}}{k_p^{eff}} z_f c_f F \frac{d\phi}{dz} \tag{17}$$

$$\frac{di}{dz} = 2ai_0 \sinh[\alpha f(\phi_{solid} - \phi)] \tag{18}$$

$$i_0 = i_0^{\text{ref}} \left(\frac{c_{O_2}}{c_{O_2}^{\text{ref}}} \right)^{\gamma_{O_2}} \left(\frac{c_{H^+}}{c_{H^+}^{\text{ref}}} \right)^{\gamma_{H^+}} \tag{19}$$

$$D_{O_2} \frac{d^2 c_{O_2}}{dz^2} - v \frac{dc_{O_2}}{dz} = -\frac{1}{4\varepsilon_m^c F} \frac{di}{dz} \tag{20}$$

In the anode catalyst layer:

$$\frac{dv_s}{dz} = 0 \tag{21}$$

$$\frac{dp}{dz} = -\frac{\mu}{k_p^{\text{eff}}} v + \frac{k_\phi^{\text{eff}}}{k_p^{\text{eff}}} z_f c_f F \frac{d\phi}{dz} \tag{22}$$

$$\frac{di}{dz} = 2ai_0 \, \sinh[\alpha f(\phi_{\text{solid}} - \phi)] \tag{23}$$

$$i_0 = i_0^{\text{ref}} \left(\frac{c_{H_2}}{c_{H_2}^{\text{ref}}} \right)^{\gamma_{H_2}} \left(\frac{c_{H^+}}{c_{H^+}^{\text{ref}}} \right)^{\gamma_{H^+}} \tag{24}$$

$$D_{H_2} \frac{d^2 c_{H_2}}{dz^2} - v \frac{dc_{H_2}}{dz} = \frac{1}{2\varepsilon_m^c F} \frac{di}{dz} \tag{25}$$

The boundary conditions or conditions of continuity must be specified at each interface. At the anode gas chamber/gas diffuser interface:

$$v_s = v_0 \tag{26}$$

$$p = p_0 \tag{27}$$

where v_0 represents the required water input at the anode in order to maintain full membrane hydration at all times. At the anode diffuser/catalyst interface:

$$v_s = v_0 + \frac{I}{2\rho F} \left(\frac{p_w^{\text{sat}}}{p_0 - p_w^{\text{sat}}} \right)$$

due to the condensation of vapor to liquid $\tag{28}$

$$c_{H_2}^{\text{sat}} = (1 - x_w) \frac{p_0}{K_{H_2}} \quad \text{according to Henry's law.} \tag{29}$$

At the anode catalyst/membrane interface:

$$\left(D_{H_2}^{\text{eff}} \frac{dc_{H_2}}{dz} \right)_c = \left(D_{H_2} \frac{dc_{H_2}}{dz} \right)_m,$$

i.e., continuous flux of dissolve hydrogen $\tag{30}$

$$c_{O_2} = 0 \quad \text{i.e., no dissolved oxygen crossover in membrane} \tag{31}$$

Similarly at the membrane/cathode catalyst layer interface:

$$c_{H_2} = 0 \tag{32}$$

$$\left[D_{O_2}^{\text{eff}} \frac{dc_{O_2}}{dz} \right]_c = \left[D_{O_2} \frac{dc_{O_2}}{dz} \right]_m \tag{33}$$

At the cathode catalyst layer/gas diffuser interface:

$$c_{O_2}^{\text{sat}} = (1 - x_w - x_{N_2}) \frac{p_L}{K_{O_2}} \tag{34}$$

At the cathode gas diffuser/gas chamber interface:

$$N_w = -\frac{I}{4F} x_w \left[1 - x_w + x_{N_2}^L \left(\frac{D^{\text{eff}}}{D^{\text{eff}}} - 1 \right) \right]^{-1} \tag{35}$$

$$p = p_L \tag{36}$$

$$x_{N_2}^L = \left(1 - \frac{p_w^{\text{sat}}}{p_L} \right) \left(\frac{x_{N_2}^0}{x_{O_2}^0} \right) \left(\frac{\xi - 1}{\xi} + \frac{x_{N_2}^0}{x_{O_2}^0} \right)^{-1} \tag{37}$$

The algorithm used to solve the given system of equations is shown in Fig. 2. The fourth order Runge–Kutta method is used to solve the equations in each region. Shooting techniques were used to obtain convergence. Three unknown terms had to be initially guessed: v_0, C_1 and C_2. C_1 and C_2 are parameters used in the solution of the second order equations in the membrane and catalyst regions. So, three convergence loops were required. The program must converge to the appropriate value of v_0 such that the pressure variable matches the end boundary conditions. Similarly, the appropriate values of C_1 and C_2 must be found for the dissolved hydrogen and oxygen values to match the given internal boundary conditions. A Newton–Raphson method was used together with the shooting technique to speed up the rate of convergence.
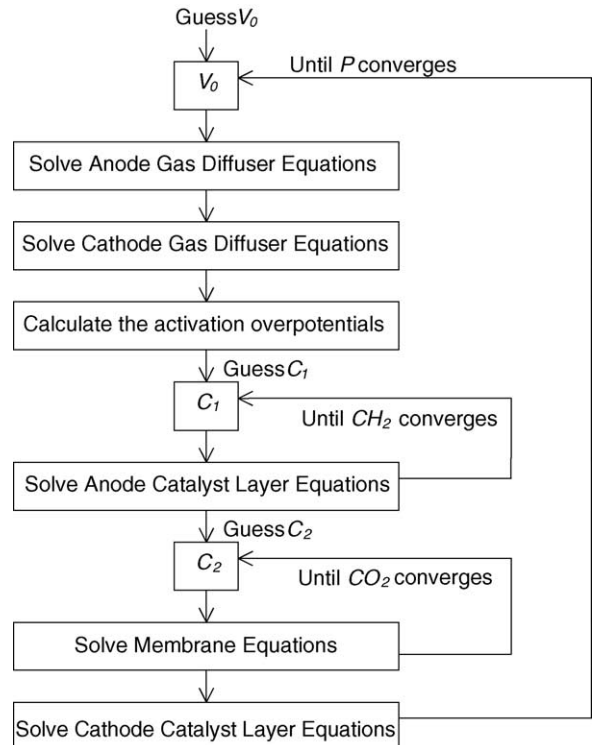

Fig. 2. Solution algorithm for the multi-domain method.

5.2. Single-domain approach

The single-domain approach consists of conservation equations, which govern the entire domain. The governing equations (38)–(53) are shown. Note all units are molar quantities.

Continuity equation:

$$\nabla(\rho\vec{v}) = S_m \tag{38}$$

where, S_m refers to the production and consumption of species at the catalyst layers.

$$S_{m,a} = S_{H_2} + S_{w,a} \quad \text{at the anode catalyst layer} \tag{39}$$

$$S_{m,c} = S_{O_2} + S_{w,c} \quad \text{at the cathode catalyst layer} \tag{40}$$

$$S_{H_2} = -\frac{I}{2F},$$

i.e., hydrogen consumed at the anode catalyst layer (41)

$$S_{O_2} = -\frac{I}{4F},$$

i.e., oxygen consumed at the cathode catalyst layer (42)

$$S_{w,a} = \frac{I}{2F}\left(\frac{p_w^{sat}}{p_0 - p_w^{sat}}\right),$$

i.e., water dissolving at the anode catalyst layer (43)

$$S_{w,c} = \frac{I}{2F}$$

i.e., water produced at the cathode catalyst layer (44)

In one-dimensional form, equations (41)–(47) are identical to equations (4), (5), (8), (9) and (17).

The momentum equation:

$$\nabla(\rho\vec{v}\vec{v} + P) + S_p = S_{m,k}\vec{v} + S_{eo} \tag{45}$$

where the source term in the momentum equation for porous media is given by Darcy's Law:

$$S_p = -\frac{\mu}{k_p}\vec{v} \tag{46}$$

The relatively small value of hydraulic permeability k_p results in the source term dominating the momentum equation and hence the problem reduces to equation (17). The electro-osmotic transport of liquid water in the membrane is given by:

$$S_{eo} = \frac{k_\phi}{k_p}z_f c_f F\nabla\phi \tag{47}$$

The transport of species H_2, O_2, N_2 and H_2O vapor are given by the following conservation equations (48)–(51):

$$\nabla(\rho\vec{v}x_{H_2}) = -\nabla(N_{H_2}) + S_{H_2} \tag{48}$$

$$\nabla(\rho\vec{v}x_{O_2}) = -\nabla(N_{O_2}) + S_{O_2} \tag{49}$$

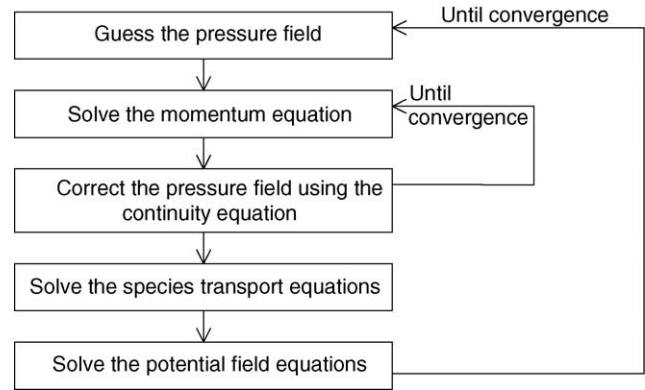$$\nabla(\rho\vec{v}x_{N_2}) = -\nabla(N_{N_2}) \tag{50}$$

Fig. 3. Solution algorithm for the single-domain method.

$$\nabla(\rho\vec{v}x_w) = -\nabla(N_w) + S_{w,a} + S_{w,c} \tag{51}$$

where the diffusion flux is given by Fick's law:

$$N_i = -\rho D_{i,j}\nabla x_i \tag{52}$$

Once again it is obvious that these are the same equations as the multi-domain approach just written in a different form. Finally the potential field equation, which accounts for ohmic and activation overpotentials, is given by:

$$\nabla(\sigma\phi) = -I + S_\varphi \tag{53}$$

where S_φ accounts for activation overpotentials at both catalyst layers.

These equations are solved using a CFD finite volume method as described in Patankar [15]. The momentum and continuity equations are solved first using the SIMPLE algorithm with a staggered grid system. In the pressure correction subroutine, the tri-diagonal matrix algorithm (TDMA) is used to speed up the solution process. Then the species equations are solved, after which the potential loss calculations are made. The whole procedure is then repeated until convergence is achieved. Fig. 3 shows the solution algorithm for the unified approach.

6. Results and discussion

In this section, results of both models are compared. The results of interest are polarization curves and water management predictions. Both models predict the voltage losses hence the net cell voltage for a given current density, and both predict the required water input and output required for maintaining full hydration of the membrane at all times.

Fig. 4 shows the polarization curves obtained using both models as well as the experimental results obtained by Ticianelli et al. [33] for the same operating conditions. Saturated hydrogen at 3 atm was used as fuel and saturated air (21% oxygen, 79% nitrogen by mole ratio) at 5 atm was used as oxidant. The cell temperature was 80 °C. Both model curves are virtually indistinguishable from each other. This is not surprising since both models solve essentially the same sets
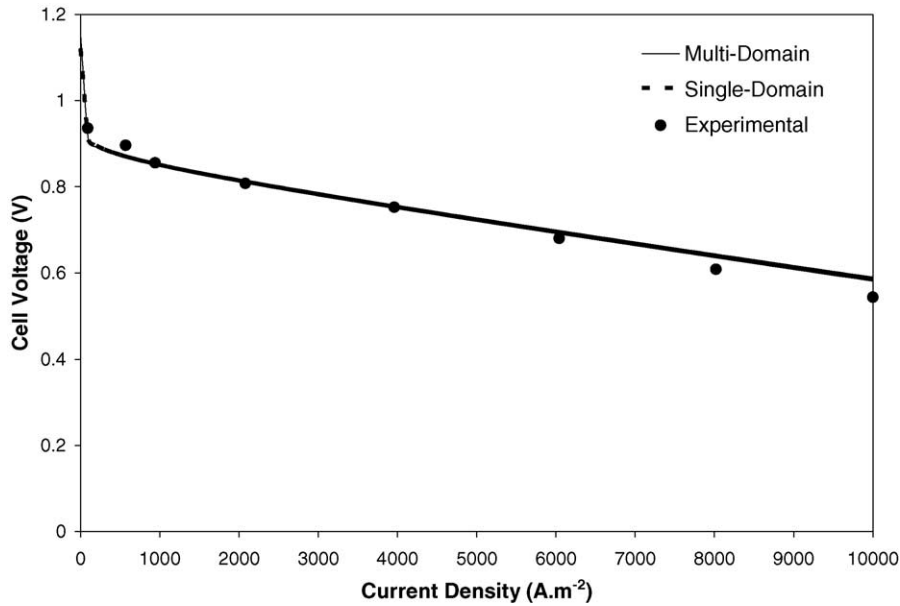
Fig. 4. Polarization curves, theoretical and experimental.

of equations, just using a different technique. Both compare well with the experimental data in the activation and ohmic overpotential regions. Both however, show signs of deviating from the experimental results at higher current densities. The reason for this is that the given model does not account for concentration overpotential, which is expected to become increasingly prominent as the current density increases.

Fig. 5 shows the water management requirements as a function of cell current density. It shows both the required input of water at the anode and the required extraction rate at the cathode for proper management, i.e., maintaining full hydra-

tion of the membrane at all times. At lower current densities liquid water flows in the reverse direction, i.e., out through the anode hence the negative values. The reason for this as explained in [11] is that at low current densities, the effects of back-pressure are larger than the effects of electro-osmotic drag. Since the cathode gas pressure is higher than the anode pressure, this pressure gradient forces the water to flow from cathode to anode. At higher current densities, the electro-osmotic effects dominate and water flows from the anode to cathode. Once again both model curves are very close. This is expected since the governing equations are essentially the same.
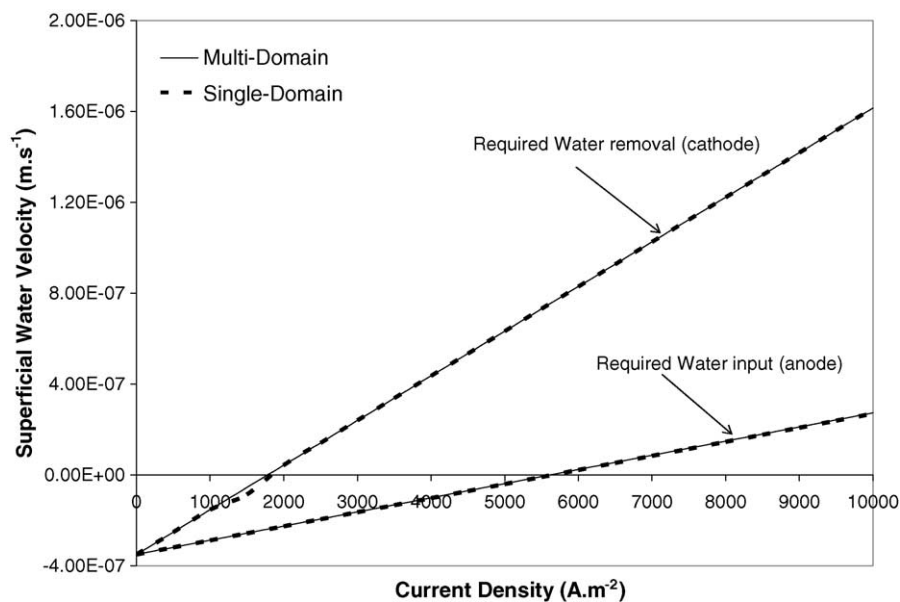

Fig. 5. Water management requirements vs. current density.

In this study, the single-domain solution converged much faster than the multi-domain solution. There are a number of reasons for this. The finite volume method used in the single-domain solution entailed a larger computational error than the single step Runge–Kutta method used in the multi-domain solution. The Runge–Kutta method requires up to four times as many calculations. Secondly, the multi-domain model treated the catalyst layer as a finite sized region whereas the single-domain model treated the catalyst layers as infinitesimally small interfaces where species are consumed and produced. For the purpose of this study, the only output parameters of interest were the polarization curves and the water management information. Therefore, the treatment of the catalyst layer (i.e., as a region or interface) was not significant. For details of the transport phenomena, the treatment of the catalyst layer would be more significant. The single-domain simply used a finer computational grid around the catalyst layers. This may have accounted for the multi-domain solution requiring extra time since the Butler–Volmer equation entails more computationally expensive calculations. So, although in this case the multi-domain solution required more computational time, it gave more precise information about species concentration in the catalyst layers. The actual convergence time for any model depends on the degree of accuracy and the efficiency of the solution algorithm. It cannot be concluded that the single-domain method is faster than the multi-domain method.

For the one-dimensional case, the solution process is much simplified. In the solutions presented in this paper, the cell current density was given and the cell voltage was calculated for that particular current density. For two- and three-dimensional cases, it is difficult to specify the cell current density since it is defined as the area integrated average across the catalyst layers. In such cases, the cell current density must be specified, but an iterative approach must be used until the area integrated average current density across the catalyst layers match the specified cell current density. Then the local overpotentials can be computed.

The most significant measure of performance of a fuel cell is the polarization curve. For PEMFCs, water management is also a critical issue. Polarization effects can be studied accurately using one-dimensional models. Comprehensive water management requires 2-D or 3-D modeling. However, a one-dimensional model can approximate the required water addition/removal required for optimum operation of the Nafion® membrane, i.e., maintaining the membrane in a fully humidified condition. Results presented here and in the literature for one-dimensional models show good agreement between theoretical and experimental polarization effects. However, one-dimensional models cannot accurately predict the spatial concentration and fluxes of species within the fuel cell. Such information is needed for the effective design and loading of catalysts. Two-dimensional models can accurately predict spatial variations in species concentration and fluxes for simple flow regimes, e.g., straight flow channels (co-flow and counter-flow arrangements). How-ever, for more complex flow regimes, such as interdigitated flow and serpentine flow channels, three-dimensional modeling is required to accurately describe the transport phenomena.

7. Conclusions

A review of recent literature in PEM fuel cell modeling was presented. Fuel cell models can be categorized as analytical, semi-empirical or mechanistic. Mechanistic models can be further subcategorized based on the solution strategy, single-domain or multi-domain. The merits and demerits of each were discussed.

The single-domain is less cumbersome in that no internal boundary conditions and conditions of continuity need to be specified. It is also easier to incorporate into commercial CFD codes. As a result, the time for model development is shortened.

The model of Bernardi and Verbrugge [11] was taken as a case study and solved using both approaches. Both models accurately predicted the polarization effects and water management requirements.

References

[1] K. Adamson, Hydrogen from renewable resources—the hundred year commitment, Energy Policy 32 (2004) 1231–1242.

[2] F. Standaert, K. Hemmes, N. Woudstra, Analytical fuel cell modeling, J. Power Sources 63 (1996) 212–234.

[3] F. Standaert, K. Hemmes, N. Woudstra, Analytical fuel cell modeling; non-isothermal fuel cells, J. Power Sources 70 (1998) 181–189.

[4] T.E. Springer, T.A. Zawodzinski, S. Gottesfeld, Polymer electrolyte fuel cell model, J. Electrochem. Soc. 138 (1991) 2334–2342.

[5] J.C. Amphlett, R.M. Baumert, R.F. Mann, B.A. Peppley, P.R. Roberge, Performance modeling of the Ballard Mark IV solid polymer electrolyte fuel cell I. Mechanistic model development, J. Electrochem. Soc. 142 (1) (1995) 1–8.

[6] L. Pisani, G. Murgia, M. Valentín, B. D'Aguanno, A new semi-empirical approach to performance curves of polymer electrolyte fuel cells, J. Power Sources 108 (2002) 192–203.

[7] G. Maggio, V. Recupero, L. Pino, Modeling polymer electrolyte fuel cells: an innovative approach, J. Power Sources 101 (2001) 275–286.

[8] S.H. Chan, S.K. Goh, S.P. Jiang, A mathematical model of polymer electrolyte fuel cell with anode CO kinetics, Electrochim. Acta 00 (2003) 1–15.

[9] C.N. Maxoulis, D.N. Tsinoglou, G.C. Koltsakis, Modeling of automotive fuel cell operation in driving cycles, Energy Conversion Manage. 45 (2004) 559–573.

[10] D.M. Bernardi, M.W. Verbrugge, Mathematical model of a gas diffusion electrode bonded to a polymer electrolyte, AIChE J. 37 (8) (1991) 1151–1163.

[11] D.M. Bernardi, M.W. Verbrugge, A mathematical model of the solid–polymer–electrolyte fuel cell, J. Electrochem. Soc. 139 (9) (1992) 2477–2491.

[12] V. Gurau, H. Liu, S. Kakac, Two-dimensional model for proton exchange membrane fuel cells, AIChE J. 44 (1998) 2410–2422.

[13] C.Y. Wang, W.B. Gu, B.Y. Liaw, Micro-macroscopic coupled modeling of batteries and fuel cells, J. Electrochem. Soc. 145 (1998) 3407–3417.

[14] T. Zhou, H. Liu, A general three-dimensional model for proton exchange membrane fuel cells, Int. J. Transport Phenomena 3 (3) (2001) 177–198.

[15] S.V. Patankar, Numerical Heat Transfer and Fluid Flow, Hemisphere, Washington DC, 1980.

[16] L. Wang, A. Husar, T. Zhou, H. Liu, A parametric study of PEM fuel cell performances, Int. J. Hydrogen Energy 28 (2003) 1263–1272.

[17] J.J. Baschuk, X. Li, Modelling of polymer electrolyte membrane fuel cells with variable degrees of water flooding, J. Power Sources 86 (2000) 181–196.

[18] S. Um, C.Y. Wang, K.S. Chen, Computational fluid dynamics modeling of proton exchange membrane fuel cells, J. Electrochem. Soc. 147 (12) (2000) 4485–4493.

[19] T. Zhou, H. Liu, A 3D model for PEM fuel cells operated on reformate, J. Power Sources, 138 (2004) 101–110.

[20] T. Berning, D.M. Lu, N. Djilali, Three-dimensional computational analysis of transport phenomena in a PEM fuel cell, J. Power Sources 106 (2002) 284–294.

[21] T. Berning, N. Djilali, Three-dimensional computational analysis of transport phenomena in a PEM fuel cell—a parametric study, J. Power Sources 124 (2003) 440–452.

[22] W.-M. Yan, F. Chen, H.-Y. Wu, C.-Y. Soong, H.-S. Chu, Analysis of thermal and water management with temperature-dependent diffusion effects in membrane of proton exchange membrane fuel cells, J. Power Sources 129 (2004) 127–137.

[23] M. Wohr, K. Holwin, W. Schurnberger, M. Fischer, W. Neubrnad, G. Eigenberger, Dynamic modeling and simulation of a polymer membrane fuel cell including mass transport limitation, Int. J. Hydrogen Energy 23 (3) (1998) 213–218.

[24] T.F. Fuller, J. Newman, Water and thermal management in solid–polymer–electrolyte fuel cells, J. Electrochem. Soc. 140 (1993) 1218–1225.

[25] S. Ge, B. Yi, A mathematical model for PEMFC in different flow modes, J. Power Sources 124 (2003) 1–11.

[26] S. Dutta, S. Shimpalee, J.W. Van Zee, Numerical prediction of mass-exchange between cathode and anode channels in a PEM fuel cell, Int. J. Heat Mass Transfer 44 (2001) 2029–2042.

[27] P.T. Nguyen, T. Berning1, N. Djilali, Computational model of a PEM fuel cell with serpentine gas flow channels, J. Power Sources 130 (2004) 149–157.

[28] S. Um, C.Y. Wang, Three-dimensional analysis of transport and electrochemical reactions in polymer electrolyte fuel cells, J. Power Sources 125 (2004) 40–51.

[29] N.P. Siegel, M.W. Ellis, D.J. Nelson, M.R. von Spakovsky, A two-dimensional computational model of a PEMFC with liquid water transport, J. Power Sources 128 (2004) 173–184.

[30] M. Hu, A. Gu, M. Wang, X. Zhu, L. Yu, Three dimensional, two phase flow mathematical model for PEM fuel cell. Part I. Model development, Energy Conversion Manage. 45 (2004) 1861–1882.

[31] M. Hu, A. Gu, M. Wang, X. Zhu, L. Yu, Three dimensional, two phase flow mathematical model for PEM fuel cell. Part II. Analysis and discussion of the internal transport mechanisms, Energy Conversion Manage. 45 (2004) 1883–1916.

[32] A. Kumar, R.G. Reddy, Modeling of polymer electrolyte membrane fuel cell with metal foam in the flow-field of the bipolar/end plates, J. Power Sources 114 (2003) 54–62.

[33] E.A. Ticainelli, C.R. Deriouin, A. Redondo, S. Srinivasan, Methods to advance technology of proton exchange membrane fuel cells, J. Electrochem. Soc. 135 (1988) 2209–2214.